Gap maps for triangular photonic crystals with a dispersive and absorbing component

Andreas Rung,[1] Carl G. Ribbing,[1] and Min Qiu[2]
[1]*Division of Solid State Physics, Department of Engineering Science, Uppsala University, Uppsala, Sweden and Department of Functional Materials, Division of Sensor Technology, Swedish Defence Research Agency, Linköping, Sweden*
[2]*Laboratory of Optics, Photonics and Quantum Electronics, Department of Microelectronics and Information Technology (IMIT), Royal Institute of Technology, Electrum 229, 164 40 Kista, Sweden*
(Received 25 April 2005; revised manuscript received 19 September 2005; published 18 November 2005)

Some consequences of a strong lattice resonance in the working frequency region of a 2D photonic crystal are investigated. It opens for two kinds of gaps in the dispersion relations: structure gaps and a polaritonic gap. A transverse optical oscillator model for ceramic beryllium oxide has been used to simulate the dielectric function of the polaritonic medium. The effective index of refraction is different on either side of the resonance, which causes BeO to act both as a high index material and a low index material. Gap maps for two kinds of triangular structures were calculated: BeO cylinders in air or in a high-index, nondispersive dielectric. These gap maps show appearance and disappearance of the transverse electric, transverse magnetic, and complete structure gaps as function of the packing fraction r/a, and the lattice constant a. The results illustrate the importance of whether the dielectric or the polaritonic material has the higher effective dielectric function. The effects of absorption, included by the damping parameter of the oscillator model, are briefly discussed.

DOI: 10.1103/PhysRevB.72.205120 PACS number(s): 42.25.Bs, 41.20.Jb, 42.79.Ci, 71.36.+c

INTRODUCTION

In this work we shall report results from detailed calculations of the photonic band structures for a 2D periodic structure with lattice constants comparable to the wavelength of infrared radiation. More specifically, one of the components in the structure will be beryllium oxide (BeO), which is characterized by an infrared band with strong absorption and dispersion caused by the excitation of transverse optical phonons in the lattice. The explicit cases will be a triangular lattice of BeO rods in air or a silicon matrix, or the corresponding inverse structures: holes of air or Si rods in a BeO matrix. The major motivation for the study is that such systems may exhibit two kinds of photonic gaps: *structural* and *polaritonic*.[1] The first kind is an effect of coherent scattering from periodically arranged structural units, while the second is a consequence of the dielectric function of the polaritonic component. In the polaritonic frequency range, i.e., $\omega_T \leqslant \omega \leqslant \omega_L$, where ω_T and ω_L are the zero wave vector frequencies of the transverse and longitudinal optical phonon branches respectively, the dielectric function is negative, which prevents propagation. This sort of structure is classified as a polaritonic photonic crystal (PPC). It is our ambition to present gap maps for this 2D PPC system as a further development of the 2D dielectric only gap maps presented by Winn *et al.*[2] Our study is limited to one specific material, but the qualitative conclusions are valid for a large group of polar compounds: oxides, carbides, nitrides, alkali halides, etc. that have a Reststrahlen band.[3]

Numerical calculations on photonic crystals (PhC) have to rely on simple models because calculations in these cases with both strong dispersion and absorption are demanding and require careful considerations.[4] There are several program packages available for calculations of photonic band structure,[5] but only some of them are suited in this case, and even then considerable attention is needed. It is interesting to compare the behavior of the two kinds of gaps when design parameters of the photonic crystals are altered. In their early work of this nature, Sigalas *et al.*[1] calculated transmittance spectra for an 8 layer slab of square structure of rods, having a gallium arsenide model dielectric function, in air. The results consistently exhibited a strong minimum around the lattice resonance, i.e., the polaritonic gap. Depending on the value of the lattice constant, the positions of the structure gaps are shifted. The authors introduced the name *twin gaps* for split structure gaps, one on each side of the polaritonic gap. Each such pair is traced back to one gap obtained with a constant dielectric function instead of the GaAs model. The clear identification of the different gaps is partly a product of using a real dielectric function, i.e., without absorption. The authors note that the introduction of absorption distorts the gap edges to an extent that may make their identification problematic. A short time after the results of Sigalas *et al.* came out, the Irvine group and collaborators managed to adapt the plane-wave method to calculations of the full 2D band structure also for situations with strong dispersion, but initially still without absorption.[6,7] The appearance of a polaritonic gap and flat bands close to ω_T was noted even for a low packing fraction of the polar component. A little later the Nanjing group managed to implement the plane wave method (PW) in a way that permitted calculation of the photonic band structure in the presence of strong dispersion.[8,9] This represents a difficulty, since solutions ω are obtained as a result of the calculations using the wave vector K as input, and at that stage the dispersive dielectric function $\varepsilon(\omega)$ is unknown. They used a model with a real $\varepsilon(\omega)$, i.e., without absorption, and even then they caution that the bands are only reliable for frequencies $\omega < \omega_T$. Their band structures include one characteristic flat band just under the polaritonic gap. This result was more developed in recent MIT work in which a new calculational method, based on vectorial eigenmode expansion, was used.[10] In this scheme, no matrix inversion is needed, so calculations around the resonance ω_T,

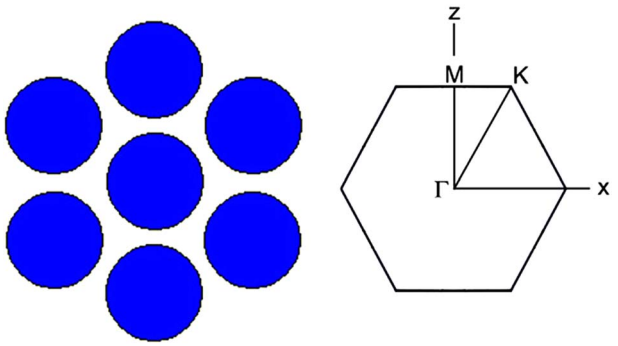

FIG. 1. (Color online) The triangular lattice (left) and the corresponding first Brillouin zone with the high symmetry points indicated (right). The y axis is perpendicular to the plane of the paper.

where the dielectric function rapidly shifts from large positive to large negative values, suffer less from numerical instability. With this method a fine structure of flat bands both below and just above ω_T was resolved. The authors also presented a detailed description of the rapid shifts in electric field pattern that occurs in a narrow frequency range around ω_T. Very recently, yet another technique was presented by Toader and John.[11] For a D-dimensional PhC the calculations are performed in a $(D+1)$-dimensional space in which the photonic band structure is obtained as the intersection between the dispersion surface and the function $\varepsilon(\omega)$. Only the case of zero absorption is considered, but it is observed that a polaritonic component from a small density of independent oscillators may synergetically enhance the photonic band gap.

TIME-DOMAIN METHOD FOR BAND STRUCTURE COMPUTATION

The band structures obtained in this work were computed by the finite-difference time-domain (FDTD) method.[12] To model polaritonic materials, time-domain auxiliary differential equations (ADEs) are utilized to link the polarization and the electric flux density.[13,14] A short description of the ADE method is given below, and the details can be found in Refs. 12–14.

The time dependent Maxwell equation is

$$\nabla \times \mathbf{H} = \frac{\partial \mathbf{D}}{\partial t} + \mathbf{J}, \tag{1}$$

where $\mathbf{J}(\omega) = \partial \mathbf{P} / \partial t$ is a polarization current used to describe the material response, and $\mathbf{P}$ is the associated time-dependent polarization. In the frequency domain, the dielectric function is described by the Lorentz model,

$$\varepsilon(\omega) = \varepsilon_\infty \left(1 + \frac{\omega_L^2 - \omega_T^2}{\omega_T^2 - \omega^2 - i\omega\gamma} \right). \tag{2}$$

Recall that the displacement field

$$\mathbf{D}(\omega) = \varepsilon_0 \varepsilon(\omega) \mathbf{E}(\omega) = \varepsilon_0 \mathbf{E}(\omega) + \mathbf{P}(\omega) \tag{3}$$

and $\mathbf{J}(\omega) = -i\omega \mathbf{P}(\omega)$ if a harmonic time dependence $e^{-i\omega t}$ is assumed. We can then equate the two expressions for $P(\omega)$:

$$i\frac{J(\omega)}{\omega} = \frac{\varepsilon_0 \varepsilon_\infty (\omega_L^2 - \omega_T^2)}{\omega_T^2 - \omega^2 - i\omega\gamma} E(\omega) \tag{4}$$

giving the equation

$$(\omega_T^2 - \omega^2 - i\omega\gamma)\mathbf{J}(\omega) = -i\omega\varepsilon_0\varepsilon_\infty(\omega_L^2 - \omega_T^2)\mathbf{E}(\omega). \tag{5}$$

Perform an inverse Fourier transformation of each term of Eq. (5) using the differentiation theorem for the Fourier transform[12–14] one then obtains

$$\frac{\partial^2 \mathbf{J}(t)}{\partial t^2} + \gamma \frac{\partial \mathbf{J}(t)}{\partial t} + \omega_T^2 \mathbf{J}(t) = \varepsilon_0 \varepsilon_\infty (\omega_L^2 - \omega_T^2) \frac{\partial \mathbf{E}(t)}{\partial t}, \tag{6}$$

which is the time-domain auxiliary differential equation. Equation (6) together with (2) can then be easily adapted in the standard FDTD method for solving the Maxwell equations.

The computational domain is chosen to be a primitive cell for a square lattice and a rectangular unit cell which contains two primitive cells for triangular lattice cases. Periodic boundary conditions, which satisfy the Bloch theorem, are used for the FDTD field components outside of the computational domain,[15] as given below, e.g., for the magnetic field:

$$H(\mathbf{r} + \mathbf{L}) = e^{ikL} H(\mathbf{r}), \tag{7}$$

where $\mathbf{k}$ is the wave vector and $\mathbf{L}$ is the lattice vector related to the primitive cell.

Special consideration should be given for the initial field distributions to excite eigenmodes of PPCs. In particular, since the computational domain contains two primitive cells for triangular lattice cases, randomly chosen initial fields could give a folded version of the band structure, containing both band structures from two primitive cells. To overcome this problem, an initial field which satisfies the Bloch theorem in both primitive cells is used in our computations.[15]

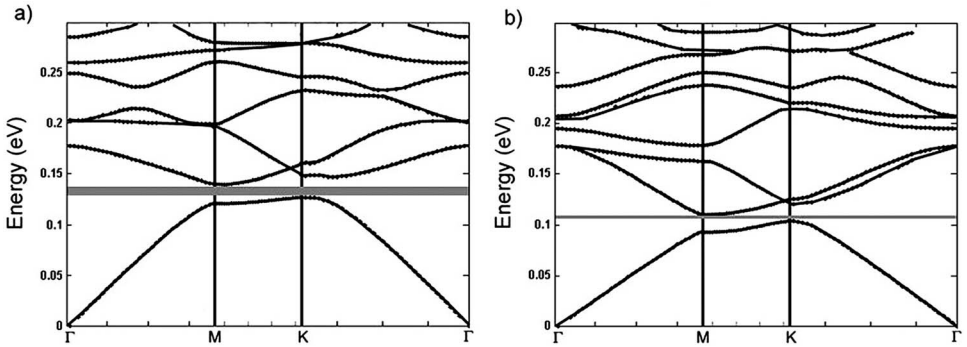

FIG. 2. The TE (a) and TM (b) band structure for a triangular lattice of dielectric cylinders, $\varepsilon = 10.6$, in an air matrix. The lattice constant is $a = 2.5\ \mu$m and the packing fraction is $r/a = 0.44$. The small omnidirectional gaps: TE around 0.135 eV and TM around 0.105 eV are shaded.

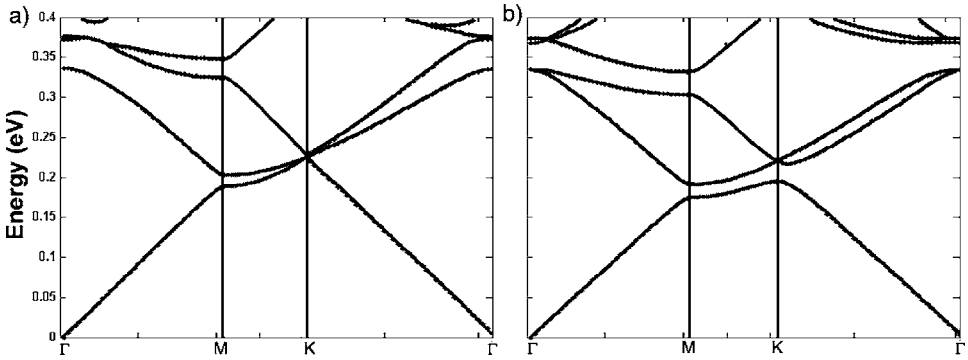

FIG. 3. The TE (a) and TM (b) band structures for a triangular lattice of dielectric cylinders, $\varepsilon = 2.99$, in an air matrix. The lattice constant $a = 2.5\ \mu$m and the packing fraction $r/a = 0.44$.

However, this safeguarding mechanism is not perfect; due to numerical problems some erroneous solutions due to band-folding from the use of a nonprimitive unit cell may appear.

For a given wave vector **k**, the electromagnetic fields starting from the initial field distributions are evolved in the time domain by the FDTD method. Fields recorded in some randomly chosen points are then Fourier transformed into the frequency domain. The peaks of the frequency spectra are eigenmodes of the PPC at the specified wave vector **k**. The band structures are thus obtained from the relation between **k** and the eigenmodes.

RESULTS AND DISCUSSION

In this work all calculations were made using the FDTD method described above. In Fig. 1 above the structure and the corresponding first Brillouin zone are shown with the conventional high symmetry point labels.

To establish a basis for comparisons we have calculated the band structures for four triangular structures of nondispersive dielectric cylinders in an air matrix and the corresponding inverse structures. Two with a highly refracting medium, $\varepsilon = 10.6$, representative for GaAs in the IR range.[16] In the other two cases we selected a lower value: $\varepsilon = 2.99$ which is the high frequency limit for the polaritonic material we want to investigate later. The lattice constant was chosen as $a = 2.5\ \mu$m and the packing fraction $r/a = 0.44$ in all four cases. The results above for the two direct structures, Figs. 2 and 3, show no complete gap, i.e., a common gap energy interval for all directions and both transverse electric (TE) and transverse magnetic (TM) modes. There are, however, separate omnidirectional gaps for the two polarizations in the high index case. These omnidirectional gaps are indicated in Fig. 2 by the shaded areas, and they are consequences of the high dielectric contrast between GaAs and air. This point is illustrated by the following band structure in Fig. 3 calculated for the lower value of the dielectric function. There are no omnidirectional gaps in these two cases because of the much lower dielectric contrast.

The band structures for the corresponding inverse cases are shown in Figs. 4 and 5. Figure 4 is remarkably different from Fig. 2 in that there is a large TE gap that fully overlaps with the TM gap that is much smaller. This growth of the TE gap when shifting to the inverse structure is in agreement with the the principle of selecting the distribution of modes between the high and low index components of the PhC that satisfies the variational principle.[17] It implies that TM modes are favoured when there is a connected lattice of low index material, and TE modes when the high index material is connected and separating islands of low index material. The corresponding low-index pair of Figs. 3 and 5 demonstrate the importance of the index contrast. In this case only the TE mode of the inverse structure has a omnidirectional gap.

With the insight that the TE and TM are favored in the inverse and direct structures, respectively, one realizes that the packing fraction plays a very important role in terms of complete photonic band gaps. First, the r/a value 0.44 is so high that the average refractive index will be lower in the inverse than in the direct structure. In the direct structure, the r/a ratio has to be large enough for the TE gaps to open, whereas it also has to be small enough to let the lattice remain connected by low index material. It was shown earlier by gap map calculations[2] that the direct structure of dielectric cylinders in a low index matrix does not exhibit a complete photonic band gap. The inverse structure with low index cylinders in a high index matrix, however, does.

The introduction of a polaritonic material into a photonic crystal has been studied previously.[1] Marked effects on the

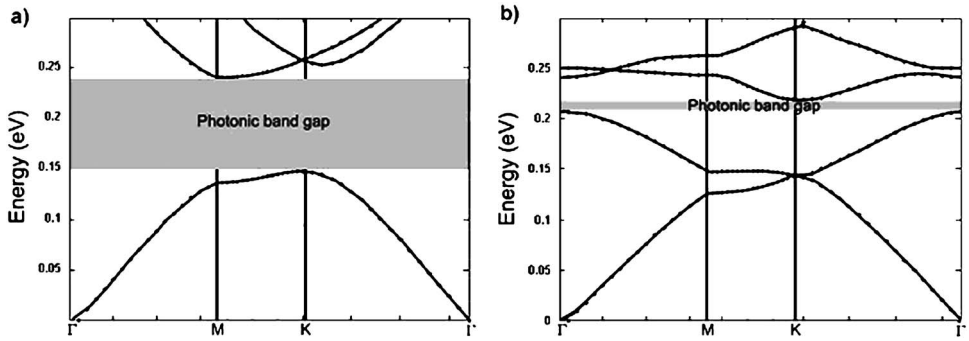

FIG. 4. The band structure for TE (a) and TM (b) modes of a triangular lattice of air holes in a dielectric matrix, $\varepsilon = 10.6$. The lattice constant is $a = 2.5\ \mu$m and the packing fraction is $r/a = 0.44$, i.e., the inverse structure of that in Fig. 2. Note the presence of a small, but complete, photonic band gap around 0.21 eV.

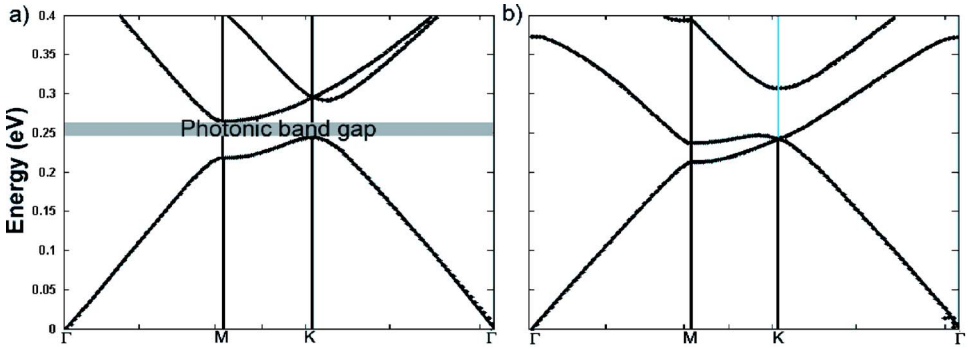

FIG. 5. (Color online) The band structure for TE (a) and TM (b) modes of a triangular lattice of air holes in a dielectric matrix, $\varepsilon = 2.99$. The lattice constant is $a = 2.5$ μm and the packing fraction is $r/a = 0.44$, i.e., the inverse structure of that in Fig. 3.

dispersion of the photonic bands was noted for filling fractions as low as $f = 0.01$.[7] Specifically it was found that as little as 1% polaritonic material in a 16 layer square photonic BeO crystal yields an optical transmittance below 20% in the polaritonic region.[18] The Lorentz one-oscillator model, given above in Eq. (2), exhibits a dramatic behavior around the resonance ω_T. The dielectric function $\varepsilon(\omega) \gg \varepsilon(0)$ when approaching ω_T from below. The dielectric function then has a pole at ω_T, which results in very large positive values of ε on the low energy side—which is "useful" in photonic crystals, since then a very large dielectric contrast can be reached in this region. At the high energy side of the pole the real part of ε is strongly negative for $\omega_T < \omega < \omega_L$, i.e., the material is optically metal-like. For $\omega > \omega_L$ it is positive, $0 < \varepsilon < \varepsilon_\infty$. This implies that the polaritonic material can act both as low and high index material in a photonic crystal, depending on the frequency. Cylinders of a polaritonic material, embedded in a dielectric matrix with $\varepsilon_\infty < \varepsilon < \varepsilon(0)$, would be the low index material above ω_L, and the high index material below ω_T. The importance of whether the polaritonic material is the high or low index material was recently discussed for a 1D photonic crystal.[19]

In this work we have focused on beryllium oxide (BeO) which is a polar material with strong dispersion around 0.1 eV. It can be modeled by the Lorentz one-oscillator model with parameters[20] listed in Table I below. The parameters given in Ref. 20 are for single crystalline BeO, which is anisotropic. In this case, we prefer to treat ceramic BeO which is isotropic, and which we have previously investigated experimentally.[21] The resonances for the parallel and perpendicular components of the electromagnetic waves have therefore been averaged in Table I. As mentioned in the Introduction, our results can be generalized to a wide group of polar compounds.

We now return to the band structure calculations and introduce BeO as one component in the photonic crystal. For a unit cell constant $a = 2.5$ μm, the photonic band gap is well separated from the polaritonic gap. For this value, and a packing fraction $r/a = 0.30$, the band structure for a triangular structure of BeO cylinders in air was calculated. The band diagrams for TE and TM modes are shown in Fig. 6 below. In this case, there are structural gaps around 0.22 eV, but none that is omnidirectional. There are, however, TE and TM gaps within the very prominent polaritonic gaps, with a small overlap. An interesting comparison to make is with the band structure for the inverse of this structure, shown below in Fig. 7, with air holes in a BeO matrix. The lattice constant and the packing fraction are unchanged. In Fig. 7 there is a small TE photonic band gap, but no TM gap, which is analogous to the dielectric case discussed above. The structure is a connected high index structure, which favors splitting of TE modes into band gaps. In the TM case the polaritonic gap is reduced in width because of penetration by bands from above in a volume around Γ.

TABLE I. Lorentz one oscillator parameters for bulk crystalline BeO, from Ref. 16. The parameters have been averaged as 1/3 of the parallel +2/3 of the perpendicular components.

Parameter	Value
ω_T	702 cm^{-1}
γ	12.2 cm^{-1}
ε_∞	2.99
$\varepsilon(0)$	7.65

At this stage another comparison between Figs. 6 and 7 with dispersion, and the non-dispersive cases in Figs. 2–5 is of interest, even if their r/a values are different. Taking the direct structures first, we notice the similarities between the behavior of bands at low frequencies $\omega < \omega_T$ in the high-index cases Figs. 2 and 6. One difference is that the introduction of the polariton gap in Fig. 6 has the effect to depress the lower energy bands further down. This is in agreement with our previous observation of interaction between photonic and polaritonic bands.[18] In the high frequency range: $\omega > \omega_L$ it is the low-index dielectric case, Fig. 3, that is similar to the dispersive case in Fig. 6, in accordance with the remarks above that a polaritonic material can act both as a high-and low-index material. Again the frequency scale is compressed in Fig. 6 because of the presence of a polaritonic gap. An analogous comparison can be made when comparing the bands for the inverse structures, i.e., Figs. 4 and 5 on one side, and Fig. 7 on the other. In Fig. 7(b), i.e., the TM mode, the low energy bands, i.e., for $\omega < \omega_T$, are strongly flattened by the polaritonic gap.

Previous work has shown that a large dielectric contrast is needed to open a complete photonic band gap. One way of achieving this is to use a triangular lattice of holes in BeO, and fill the holes with a dielectric such as GaAs ($\varepsilon = 10.6$) or Si ($\varepsilon = 16.0$)—cases to which we will return below.

We shall briefly discuss the influence of the absorption in the polaritonic component. The absorption enters via the Lorentz parameter γ which makes $\varepsilon_2(\omega)$ nonzero. In Figs. 6 and 7 we have used the tabulated value for γ, given in Table I,

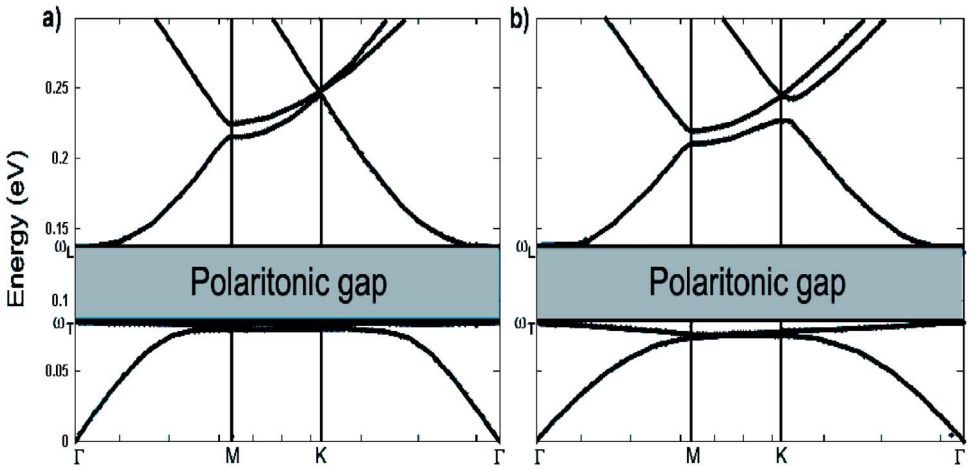

FIG. 6. (Color online) The TE (a) and TM (b) band structures for a triangular lattice of BeO cylinders in air. The lattice constant $a=2.5$ μm and the packing fraction $r/a=0.30$. The polaritonic gap is situated between the frequencies ω_T and ω_L, which are indicated by horizontal lines.

which is much less than the resonance ω_T. This implies that the resonance is "sharp" and the dispersion strong, as alluded to above. This sharpness is of importance for the appearance of flat bands, which is both of fundamental interest and a difficulty in numerical calculations. It follows from the dispersion relation

$$\omega = \frac{cK}{\sqrt{\tilde{\varepsilon}(\omega)}} \tag{8}$$

that a strictly flat band, i.e., $d\omega/dK=0$, appears when ε is real and $\to\infty$. This corresponds to ω_T being a true pole, zero damping and no absorption. In FDTD-calculations cases with strong dispersion require calculations with high time resolution in order to have sufficient frequency resolution after the Fourier transformation. It is difficult to quantify the resulting frequency resolution given an initial choice of time steps, and it is furthermore obvious that in this particular respect FDTD calculations cannot compete with the vectorial eigenmode expansion method for which this problem is not serious. We thus cannot hope to obtain the fine structure of horizontal bands as calculated with the CAMFR-method.[10]

So far we have shown two different band structures where a polaritonic material acts as one component of the photonic crystal, either the cylinders or the matrix. We have also discussed the importance of the packing fraction for complete gaps to open. If these two variations are combined, and the TE and TM gaps are collected for various packing fractions, we obtain a *gap map*. A gap map for the triangular structure of BeO cylinders in air is shown below. The lattice constant $a=2.5$ μm is kept constant, whereas the packing fraction was varied.

In Fig. 8 one can note the existence of a TM photonic band gap for moderate packing fractions, and also the increase of the TM gaps as the packing fraction increases. The overlap between the photonic gaps inside the polaritonic gap appears at a packing fraction $r/a=0.26$, and remains open even for a close packed structure, $r/a=0.50$.

We now compare the pattern in Fig. 8 with the corresponding results for a dielectric-only photonic crystal: Fig. 5 in Ref. 2. Our results show one structural TM gap around 0.25 eV which corresponds to 0.5 in normalized units. The dielectric results include many gaps going to higher energies, and furthermore the dielectric constant of the matrix has a different value. Nevertheless, our TM gap corresponds fairly well in slope and shape with the lower TM gaps for the dielectric case.[2] In contrast, the TM and TE areas obtained inside the polaritonic range are almost horizontal. The polaritonic effect is to rotate them and "squeeze" them together, thus giving the complete gap shown. A possible interpretation of their horizontal orientation is that close to ω_T the dielectric function assumes such high values that the variation of r/a is of minor importance.

For the inverse case, a corresponding gap map was constructed and is reproduced in Fig. 9. Again, the symmetry is

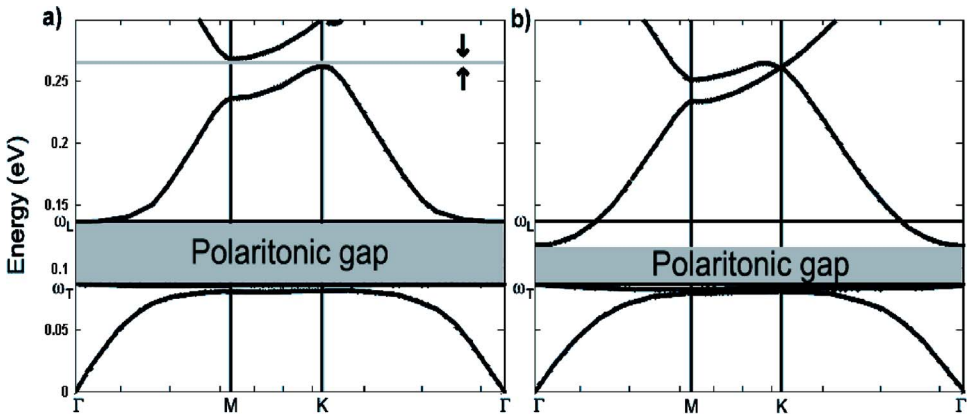

FIG. 7. (Color online) The band structure for TE (a) and TM (b) modes of a triangular lattice of air holes in a BeO matrix. The lattice constant $a=2.5$ μm, and the packing fraction $r/a=0.30$. The small TE photonic band gap has been indicated in diagram (a).

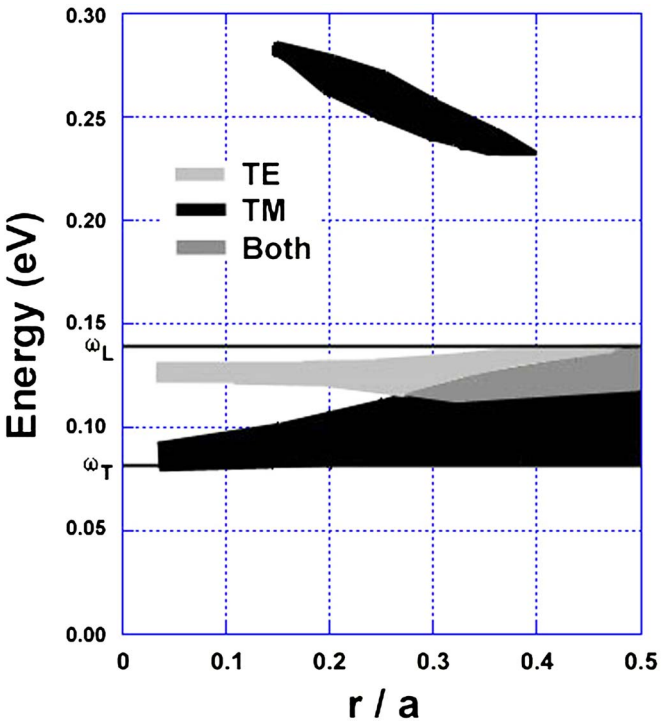

FIG. 8. (Color online) A gap map showing the TE and TM gaps as a function of packing fraction, r/a, for a triangular lattice of BeO cylinders in air. The lattice constant $a=2.5$ μm was kept constant.

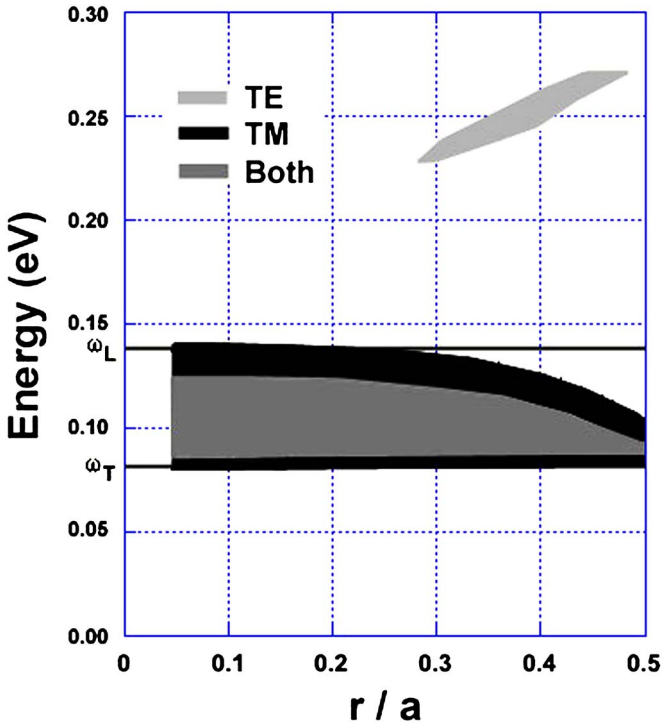

FIG. 9. (Color online) A gap map for an inverse triangular structure: Air holes in a BeO matrix. The lattice constant $a=2.5$ μm was kept constant.

triangular, and the lattice constant is $a=2.5$. The overall shapes are very different: the gap widths inside the polaritonic gap decrease with increased packing fraction. We also note the presence of a TE photonic band gap. In this case an increase in packing fraction yields less polaritonic material, hence the decrease in gap size. Again, comparing with the dielectric case, Fig. 6 in Ref. 2: the slope and shape of the TE gap areas are similar. However, in the polaritonic area, the structure gaps grow in width with increasing packing fraction.

To achieve a complete photonic band gap, the previous structure was replaced with a similar structure of BeO cylinders in a high index dielectric matrix. For $a=2.5$ μm and $r/a=0.44$, the band structure for a triangular lattice of BeO cylinders in a dielectric with $\varepsilon=10.6$ was calculated. The band diagrams for TE and TM modes are shown in Fig. 10 below. In comparison with Fig. 6, we notice closing of the TM gap and the opening of an omnidirectional TE gap. In this case, the matrix acts as high index material at energies above the polaritonic gap since $\varepsilon_\infty < 10.6$. The appearance of a large TE gap is not surprising since the cylinders, i.e., the low index material, forms isolated "islands" in the high index surrounding. However, if the matrix dielectric constant is increased further, a TM gap will open up again due to the increased contrast in ε, and we obtain a small complete gap. This is shown in Fig. 11 below where $\varepsilon=16.0$, typical for Si in the thermal infrared range.

To investigate the behavior of this complete gap, a gap map for this case was constructed. Figure 12 gives the gap map for the triangular lattice of BeO cylinders in a dielectric matrix with $\varepsilon=16.0$. The lattice constant is $a=2.5$ μm. In this case, some structure gaps are above the polaritonic gap. If, for a given r/a value, the lattice constant a is increased, these structure gaps will shift to lower energies and approach the polaritonic range. A new gap map to illustrate this process can be created. It shows the interaction between the structure gaps and the polaritonic gap, and some interesting

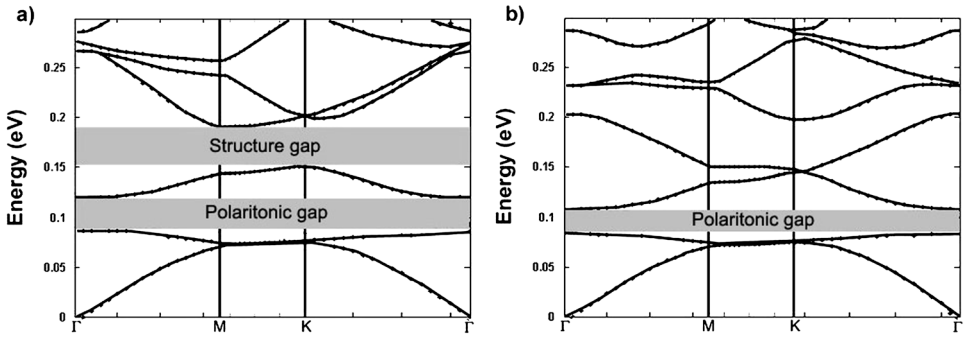

FIG. 10. (Color online) TE (a) and TM (b) band structures for a triangular photonic crystal with lattice constant $a=2.5$ μm, $r/a=0.44$ consisting of BeO cylinders in a dielectric matrix, $\varepsilon=10.6$. Note the presence of an omnidirectional TE gap.

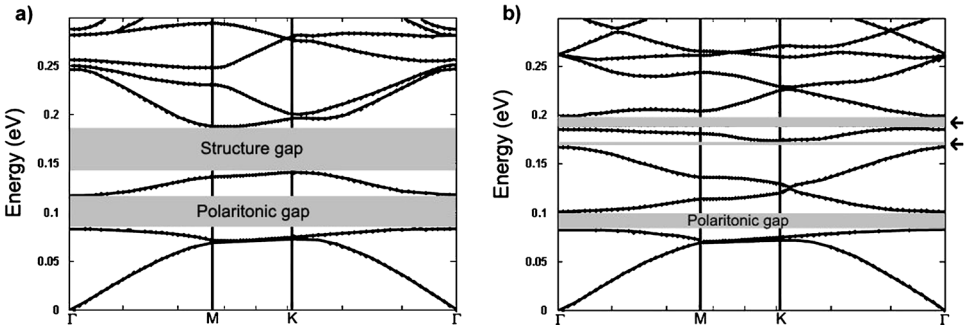

FIG. 11. (Color online) TE (a) and TM (b) band structures for a triangular lattice of BeO cylinders embedded in a dielectric, $\varepsilon=16.0$. The lattice constant $a=2.5$ μm, and $r/a=0.44$. In (b) the photonic band gaps are indicated with arrows. Note the overlap between the lowest TM and the TE structure gaps—i.e., a complete gap.

features appear in Fig. 13 with a packing fraction $r/a=0.46$. We observe for small a values the two complete gaps at high energies indicated in Fig. 12. At larger a values and for energies just above ω_L, there are complete gaps for ranges of a values up to $a=7$ μm. The wide TE gap progressively moves into the polaritonic gap for a values in the range 3–7.5 μm. The narrower TM gaps drop steeper, except for the low-lying TM gap just above ω_T that does not shift in the a range 2.5–4.5 μm. The structure gaps reappear below ω_T and merge to a large area with a complete gap that is only weakly a dependent. At energies slightly below ω_T, the dielectric function of BeO is very large—which makes the $\varepsilon=16.0$ matrix act as the low index material—and thus the much wider TM gap, as discussed previously.

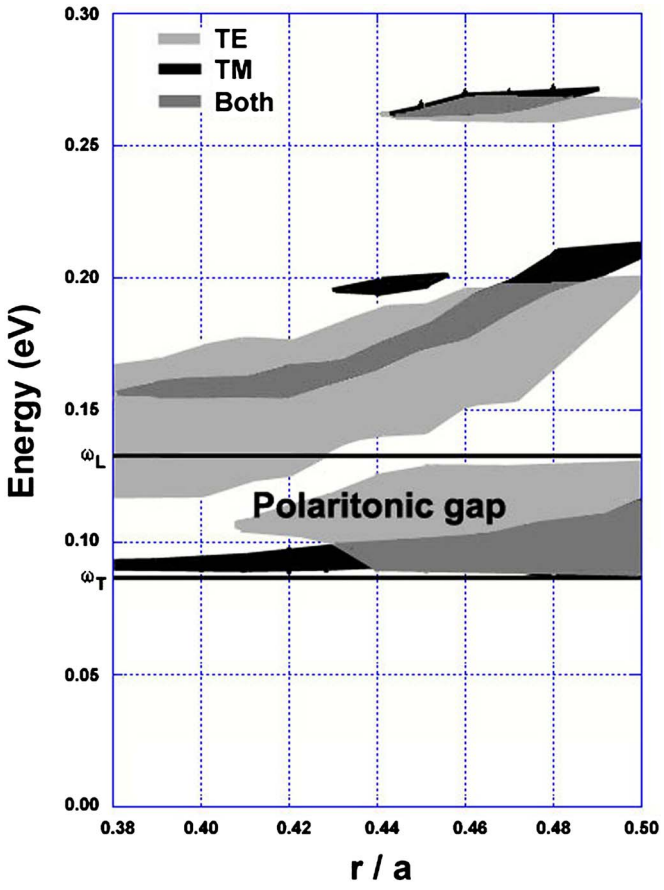

FIG. 12. (Color online) A gap map of TE and TM gaps in a triangular lattice of BeO cylinders embedded in an $\varepsilon=16.0$ matrix. The lattice constant $a=2.5$ μm, and the packing fraction was varied in small steps from 0.38 to 0.50, the region where the complete gaps were found in the calculations. The polaritonic gap is indicated.

SUMMARY AND CONCLUSIONS

In this work, we have studied the behavior of a polaritonic gap and structure gaps in triangular photonic crystals. Where meaningful comparisons can be made we have discussed earlier results for triangular, dielectric-only photonic crystals.[2] The polaritonic material in our case has been BeO, it is dispersive and has a strong resonance around 0.1 eV. The dielectric function is very different on the two sides of this resonance. For frequencies lower than ω_T, the dielectric function is large and positive near the resonance, but decreases towards $\varepsilon(0)=7.65$ for lower frequencies. On the other side of the resonance, $\varepsilon(\omega)<0$ for an interval in which it exhibits metal-like properties—this is the polaritonic gap. Above the frequency where $\varepsilon(\omega)=0$, denoted ω_L, the dielectric function increases towards $\varepsilon_\infty=2.99$. Thus, over a large

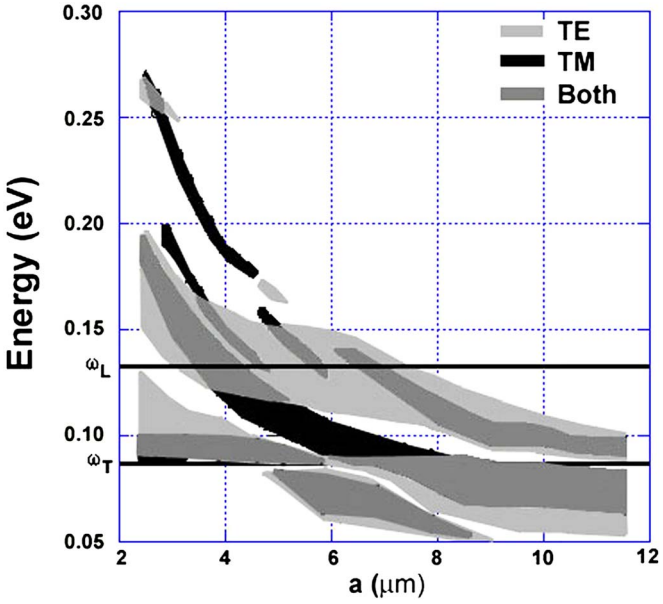

FIG. 13. (Color online) A gap map showing the photonic gap interactions with the polaritonic gap. The lattice constant was varied from 2.5 to 11.6 μm, whereas the packing fraction remained constant $r/a=0.46$. The structure is a triangular lattice of BeO cylinders embedded in a dielectric matrix with $\varepsilon=16.0$.

frequency interval, including the resonance frequency, the refractive index contrast is strongly varying. We have noticed in several cases that, just like in a 1D case, it is of importance whether the polaritonic material is on "the average" the high or low index material in comparison to the matrix.[19] A polaritonic material such as BeO can act as the high index material at all frequencies below ω_T and above ω_L, and are metal-like in between. We have therefore compared the BeO PPC's with two different nondispersive dielectric cases and noticed that the high index case show similarities with the $\omega < \omega_T$ behavior of the PPC, while the $\omega > \omega_L$ region is in better agreement with the dielectric case having $\varepsilon = \varepsilon_\infty$.

A gap map shows the polaritonic and the structure gaps as a function of packing fraction, r/a. No complete gap except for the polaritonic was obtained. Secondly, the inverse case was studied: air holes in a BeO matrix, and as in the first case no complete structure gaps were present. In the third case, the BeO cylinders were embedded in a dielectric matrix with $\varepsilon = 10.6$, and calculations on the structure with lattice constant $a = 2.5$ μm and a packing fraction $r/a = 0.46$. This resulted in a large TE structure gap, but no TM gap outside the polaritonic gap. The dielectric function of the matrix was increased further to $\varepsilon = 16.0$ and then the corresponding gap map shows the presence of a complete photonic gap for packing fractions $0.38 < r/a < 0.48$. In this case, it was also investigated in what fashion the complete structure gap shifts across the polaritonic gap. To achieve this, the packing fraction was kept constant at $r/a = 0.46$, whereas the lattice constant was increased from 2.5 to 11.8 μm. The TE and TM gaps then shifted down in energy into the polaritonic gap.

ACKNOWLEDGMENTS

A. R. and C-G.R. gratefully acknowledge sponsoring by The Swedish Research Council (VR) under contract 2002-5000 and the Swedish Defence Research Agency through the Linköping laboratory. M.Q. is grateful for support from the Swedish Foundation for Strategic Research (SSF) on INGVAR program, the SSF Strategic Research Center in Photonics, and the Swedish Research Council (VR) under project 2003-5501.

[1] M. M. Sigalas, C. M. Soukoulis, C. T. Chan, and K. M. Ho, Phys. Rev. B **49**, 11080 (1994).
[2] J. N. Winn, R. D. Meade, and J. D. Joannopoulos, J. Mod. Opt. **41**, 257 (1994).
[3] J. Dobrowolski, in *Handbook of Optics*, edited by W. Driscoll and S. Vaughan (McGraw-Hill, New York, 1978), Chap. 8, Sec. 99.
[4] A. A. Maradudin, V. Kuzmiak, and A. R. McGurn, in *Photonic Band Gap Materials*, edited by C. M. Soukoulis (Klüwer Acad. Publ, London, 1995), pp. 271–339.
[5] E.g. http://ab-initio.mit.edu/mpb/, http://www.elec.gla.ac.uk/~areynolds, http://camfr.sourceforge.net/
[6] A. R. McGurn and A. A. Maradudin, Phys. Rev. B **48**, 17576 (1993).
[7] V. Kuzmiak, A. A. Maradudin, and A. R. McGurn, Phys. Rev. B **55**, 4298 (1997).
[8] W. Zhang, A. Hu, X. Lei, N. Xu, and N. Ming, Phys. Rev. B **54**, 10280 (1996).
[9] W. Zhang, A. Hu, and N. Ming, J. Phys.: Condens. Matter **9**, 541 (1997).
[10] K. C. Huang, P. Bienstman, J. D. Joannopoulos, K. A. Nelson, and S. Fan, Phys. Rev. B **68**, 075209 (2003).
[11] O. Toader and S. John, Phys. Rev. E **70**, 046605 (2004).
[12] A. Taflove, *Computational Electrodynamics: The Finite-Difference Time-Domain Method* (Artech House INC, Norwood, 1995).
[13] T. Kashiwa and I. Fukai, Microwave Opt. Technol. Lett. **3**, 203 (1990).
[14] R. M. Joseph, S. C. Hagness, and A. Taflove, Opt. Lett. **16**, 1412 (1991).
[15] C. T. Chan, Q. L. Yu, and K. M. Ho, Phys. Rev. B **51**, 16635 (1995).
[16] E. D. Palik, in *Handbook of Optical Constants of Solids*, edited by E. D. Palik (Academic Press, New York, 1985), p. 429.
[17] J. D. Joannopoulos, R. D. Meade, and J. N. Winn, *Photonic Crystals* (Princeton University Press, Princeton, NJ, 1995).
[18] A. Rung and C. G. Ribbing, Phys. Rev. Lett. **92**, 123901 (2004).
[19] H. Högström and C. G. Ribbing, Photonics Nanostruct. Fundam. Appl. **2/1**, 23 (2004).
[20] D. F. Edwards and R. H. White, in *Handbook of Optical Constants of Solids II*, edited by E. D. Palik (Academic Press, New York, 1991), p. 805.
[21] T. Chibuye, C. G. Ribbing, and E. Wäckelgård, Appl. Opt. **33**, 5975 (1994).